JOURNAL OF APPLIED ELECTROCHEMISTRY 24 (1994) 1139–1145

Corrosion inhibition of amorphous FeBSiC alloy in 1 M HCl by 3-amino-1,2,4-triazole

S. KERTIT*

Laboratoire de Physico-Chimie des Matériaux, Ecole Normale Supérieure de Takaddoum, BP 5118, Rabat, Morocco

F. CHAOUKET

Laboratoire d'Electrochimie-Corrosion, Faculté des Sciences de Rabat, Morocco

A. SRHIRI

Laboratoire d'Electrochimie, Faculté des Sciences de Kénitra, Morocco

M. KEDDAM

Laboratoire de Physique des Liquides et Electrochimie UPR15 du CNRS, Université Pierre et Marie Curie, 4 place Jussieu, tour 22, 75252 Paris, Cedex 05, France

Received 16 February 1994; revised 11 April 1994

The mode of corrosion inhibition of amorphous FeBSiC alloy due to 3-amino-1,2,4-triazole (ATA) in molar HCl is studied through weight loss and electrochemical steady-state and transient measurements. From the comparison of results with those obtained using other 'triazole' type-organic compounds, it is shown that ATA is the best inhibitor. ATA acts on the cathodic reaction without changing the mechanism of the hydrogen evolution reaction. Impedance studies show that ATA acts by formation of a 3D compact and protective adsorbed inhibition film at the metal surface which is similar to a paint or polymer film. A correlation between the inhibition efficiency of ATA and its molecular structure is established. A schematic representation of surface coverage due to different adsorption modes of ATA is presented. The schematic representation proposed explains why the mechanism of hydrogen reduction is the same in the absence and in the presence of ATA.

1. Introduction

Metal-metalloids, metallic glasses prepared by rapid quenching from the liquid state (meltspinning) exhibit better magnetic [1–4] and high mechanical strength [5–7] properties and, in some cases, have outstanding corrosion resistance. Since the first report in 1974 on the corrosion behaviour of metallic glasses [8], many studies on electrochemical corrosion properties of amorphous alloys have been conducted. After two decades of research in this field, the existing data show that the excellent corrosion resistance of some amorphous alloys is due to their specific chemical composition and not predominantly due to their disordered structure [9–12].

It is known that the iron, nickel, and cobalt-base amorphous alloys, with no other metallic elements such as chromium, show poor corrosion resistance in different media [13–16]. However, amorphous alloys containing chromium and phosphorus are characterized by extremely high corrosion resistance, even in hot concentrated hydrochloric acid. Some of these amorphous alloys become spontaneously passive and show no pitting [17–25]. This behaviour has been attributed to the presence of highly homogeneous, stable and protective passive films, mainly formed by hydrated chromium oxyhydroxide [26, 27].

We have already reported that amorphous FeBSi and FeBSiC alloys exhibit extremely poor corrosion resistance in 1 M HCl [28–32]. The improvement of corrosion resistance of these alloys by addition of disulfide type-organic compounds has been studied [28–32]. In the present work, we have studied the effect of addition of 3-amino-1,2,4-triazole (ATA) on the corrosion resistance of the amorphous FeBSiC alloy in 1 M HCl. The corrosion inhibition due to ATA is compared to the action of other organic compounds of the same family, such as benzotriazole (BZT) and 1,2,4-triazole (TA) (Fig. 1). This research was stimulated by the successful application of triazole type-organic compounds as corrosion inhibitors for copper and iron [33–39].

The electrochemical behaviour of the interface FeBSiC/1 M HCl in the absence and in the presence, of ATA has been studied through potentiokinetic

* Author to whom correspondence should be addressed.

0021-891X

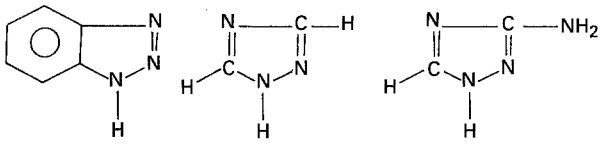

Benzotriazole (BZT) 1,2,4-triazole (TA) 3-amino-1,2,4-triazole (ATA)

Fig. 1. Molecular structure of triazole-type organic compounds studied.

polarization methods and gravimetric and electrochemical impedance measurements.

2. Experimental details

The electrochemical cell used has been described previously [28]. The amorphous $Fe_{80}B_{13}Si_{3.5}C_{3.5}$ (at %) alloy studied was prepared at CNRS-VITRY by the high speed quench technique (melt spinning). Its amorphous structure has been confirmed using X-ray diffraction and differential thermal analysis [29]. The working electrode in the form of a disc cut from the amorphous tape, had a surface area of 0.70 cm^2. The electrochemical measurements were made on the bright face of the working amorphous electrode. A saturated calomel electrode (SCE) and platinum electrode were used as reference and auxiliary electrodes, respectively.

The aggressive solutions (1 M HCl) were prepared by dilution of analytical grade 37% HCl with bidistilled water. All tests were performed at room temperature in magnetically stirred and deaerated solutions. The triazole compounds tested as inhibitors were 'Fluka' commercial products.

Electrochemical steady-state and weight loss measurements were carried out under experimental conditions described elsewhere [28, 29].

Electrochemical impedance tests were made in unstirred and deaerated 1 M HCl at room temperature, by using a transfer function analyser (Schlumberger Solartron 1250), a potentiostat (Solartron 1286) and a personal computer. Sine wave voltages (10–20 mV r.m.s.) at frequencies between 100 kHz to 10 mHz with five frequencies per decade were adopted. The measurements were automatically controlled with the aid of the developed programs. The impedance diagrams for the frequencies studied are presented as Nyquist plots where R is the real and $-jG$ the imaginary part.

Prior to electrochemical and gravimetric measurements, the amorphous sample was cleaned with acetone, thoroughly washed with bidistilled water and finally dried in dry air.

3. Results

3.1. *Comparative study*

The cathodic potentiokinetic polarization curves of amorphous FeBSiC alloy in molar HCl in the absence and presence of triazole type-organic

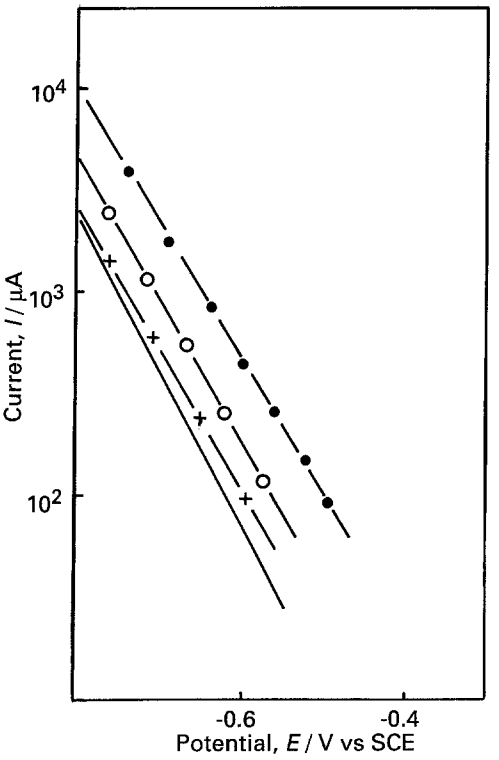

Fig. 2. Cathodic current–potentials curves of the amorphous FeBSiC alloy in molar HCl and in molar HCl + 10^{-2} M of different triazole compounds. 1 M HCl (●), TA (○), BZT (+), ATA (——). The area of working electrode is 0.70 cm^2.

compounds at 10^{-2} M are represented in Fig. 2. Values of associated electrochemical parameters and corrosion inhibition efficiency (E%) are given in Table 1. The percentage inhibition efficiency is defined as

$$E = (1 - I_{cor}/I'_{cor}) \times 100 \qquad (1)$$

where I_{cor} and I'_{cor} are the uninhibited and inhibited corrosion current densities, respectively, determined by extrapolation of cathodic Tafel lines. The values of E(%) were compared with those of E(%) obtained by the weight loss method [29] (Table 1).

As can be seen from Fig. 2, current–potential curves gave rise to parallel Tafel lines indicating that the hydrogen evolution reaction is activation controlled and the addition of triazoles does not modify the mechanism. The addition of organic compounds decreases the cathodic current with respect to the uninhibited case. The value of corrosion potential is not modified by addition of triazoles.

Table 1. Electrochemical parameters of the amorphous FeBSiC alloy in 1 M HCl; in 1 M HCl + added different triazole products at 10^{-2} M and the corresponding corrosion efficiency determined from extrapolation of Tafel lines (E_1) and gravimetric measurements (E_2)

Electrolyte	E_{cor} /mV vs SCE	I_{cor} /μA cm^{-2}	b_c /mV $(dec)^{-1}$	E_1	E_2
1 M HCl	−450	94	165	–	–
1 M HCl + 10^{-2} M TA	−440	25	160	70	60
1 M HCl + 10^{-2} M BTA	−440	12	170	85	80
1 M HCl + 10^{-2} M ATA	−440	06	150	94	90

According to Table 1, the maximum of inhibition efficiency is obtained in the presence of ATA. The corrosion inhibition efficiency of triazoles decrease in the order ATA > BZT > TA. As a result of this classification and in order to better understand the inhibition mechanism of ATA, a detailed study on this compound was carried out.

3.2. *Detailed study of ATA*

3.2.1. Electrochemical steady-state and weight loss measurements. Figure 3 shows cathodic current-potential curves of the amorphous FeBSiC alloy in 1 M HCl in the absence and presence of ATA, at different concentrations varying from 10^{-5} to 10^{-2} M. It is clear that the cathodic reaction (hydrogen evolution) is inhibited and the inhibition increases as the inhibitor concentration increases. Tafel lines of approximately equal slope were obtained. The constancy of this cathodic slope indicates that the mechanism of the proton discharge reaction does not change in the presence of ATA.

Values of corrosion current densities (I_{cor}), corrosion potential (E_{cor}), cathodic Tafel slope (b_c) and corrosion inhibition efficiency determined by polarization and gravimetric methods as a function of ATA concentrations are given in Table 2. From this table, it can be concluded that:

(i) I_{cor} decreases with increasing inhibitor concentration.

(ii) Addition of ATA does not change the values of E_{cor} and b_c.

(iii) $E(\%)$ increases with inhibitor concentration, reaching a maximum at 10^{-2} M ATA. $E(\%)$ values determined by the two methods are in reasonably good agreement.

Table 2. Electrochemical parameters of the amorphous FeBSiC alloy in 1 M HCl; in 1 M HCl + added different concentrations of ATA and the corresponding corrosion efficiency determined from extrapolation of Tafel lines (E_1) and gravimetric measurements (E_2)

ATA concentration /M	E_{cor} /mV vs SCE	I_{cor} /μA cm^{-2}	b_c /mV (dec)$^{-1}$	E_1 /%	E_2 /%
0	−450	94	165	–	–
10^{-5}	−450	56	160	40	60
10^{-4}	−454	28	155	70	75
10^{-3}	−445	14	150	85	83
10^{-2}	−440	06	150	94	90

The anodic polarization curves of amorphous FeBSiC alloy in 1M HCl and in 1 M HCl + 10^{-2} M ATA are given in Fig. 4. For overvoltages higher than −200 mV vs SCE, the presence of ATA does not change the current–potential characteristics. This means that the inhibition mode of ATA depends on electrode potential. The inhibitor has little effect when the potential becomes more positive than E_{cor}. This indicates that ATA predominates as a cathodic inhibitor.

3.2.2. Electrochemical impedance measurements. To obtain a better understanding of the interaction mechanism between ATA molecules and the amorphous FeBSiC alloy in 1 M HCl, impedance galvanostatic measurements at zero total current at the interface were carried out. Nyquist plots obtained at the interface in the absence and presence of 10^{-2} M ATA after 40 min at E_{cor} prior to the

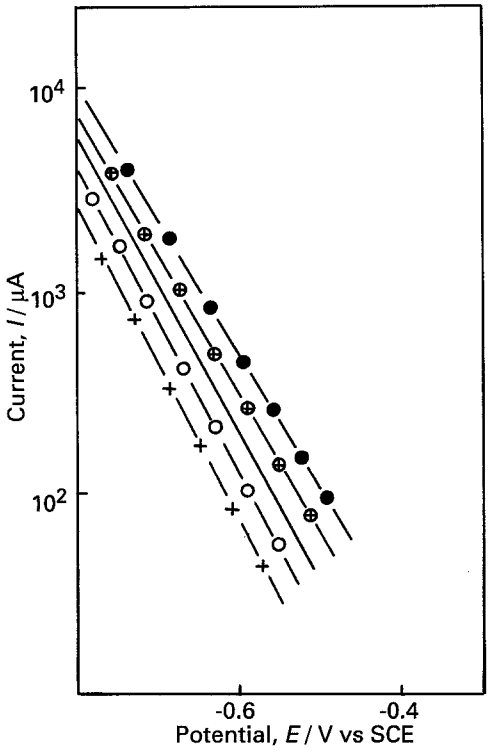

Fig. 3. Potentiokinetic polarization curves of amorphous FeBSiC alloy in 1 M HCl in the presence of different concentrations of ATA inhibitor. (●) 0.0; (⊕) 10^{-5}; (——) 10^{-4}; (○) 10^{-3}; (+) 10^{-2} M. The area of working electrode is 0.70 cm^2.

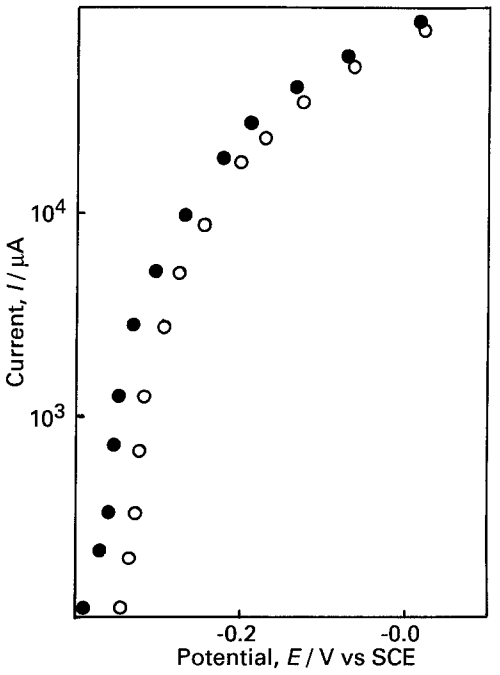

Fig. 4. Anodic current–potentials characteristics of the amorphous FeBSiC alloy in 1 M HCl (●) and in 1 M HCl + 10^{-2} M ATA (○). The area of working electrode is 0.70 cm^2.

measurements are represented in Figs 5 and 6, respectively.

The impedance diagram obtained with 1 M HCl (Fig. 5) shows only one depressed capacitive loop. At low frequencies, the presence of capacitive and inductive loops can be attributed to adsorption of species resulting from alloy dissolution and to the adsorption of hydrogen [40, 41].

In 1 M HCl + 10^{-2} M ATA, the impedance diagram is characterized by an increase of polarization resistance R_p and the appearance of two well-separated capacitive loops (Fig. 6). In fact, one first loop appears at high frequencies. The associated characteristic frequency (f_{HF}) is very high (about 10 kHz). On the other hand, this loop does appear in the uninhibited case (Fig. 5). The high frequency loop may thus be due to the presence of a dielectric film of ATA at the metal/1 M HCl interface. The resistance value associated with this loop 'HF' (R_{HF}) is around 20 Ωcm^2. This is very low and cannot be attributed to charge transfer. On the other hand, if this loop (HF) were attributed to charge transfer, so as $R_{HF} < R_T$ (uninhibited) would mean that the amorphous alloy corrodes faster in the presence of ATA. This hypothesis is in conflict with the large inhibition efficiency (94%) obtained by gravimetric and steady state measurements. This would also be in conflict with the absence of surface corrosion products in the presence of ATA. The capacity associated with the HF loop is determined by the relationship $C_{HF} = (2\pi R_{HF} f_{HF})^{-1}$; its value is about 0.8 $\mu F cm^{-2}$. This value is too low to correspond to a double layer (50–100 $\mu F cm^{-2}$).

The second capacitive loop 'LF' appears at low frequencies. It is similar to the capacitive loop obtained for the uninhibited case and may be attributed to charge transfer. Comparison of impedance diagrams (Figs 5 and 6) shows that ATA action is illustrated by modification of the impedance diagrams (appearance of two capacitive loops, increase in polarisation resistance, disappearance of the inductive loop which appears in the untreated electrode).

The characteristic parameters of the two loops are given in Table 3.

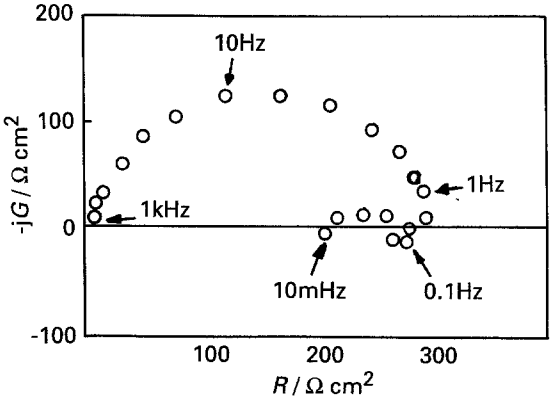

Fig. 5. Electrochemical galvanostatic impedance diagram of the amorphous FeBSiC alloy electrode in 1 M HCl after 40 min immersion at E_{cor} prior to measurements.

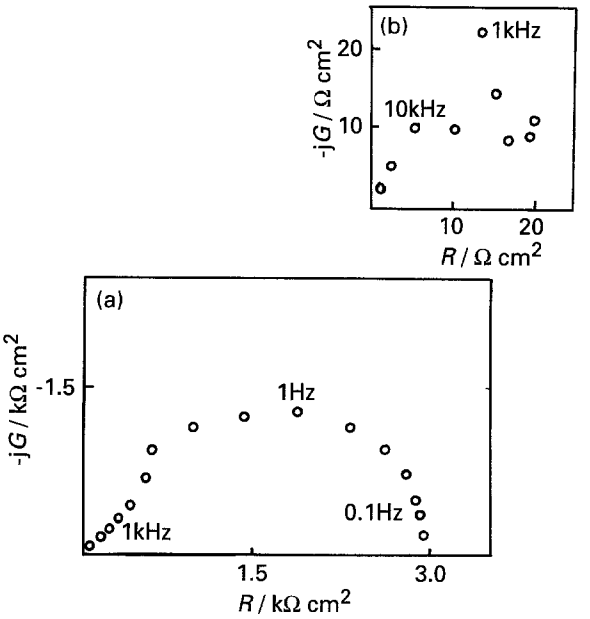

Fig. 6. (a) Electrochemical galvanostatic impedance diagram of the amorphous FeBSiC alloy electrode in 1 M HCl + 10^{-2} M ATA after 40 min immersion at E_{cor} prior to measurements; (b) represents the HF range of (a) on expended scale.

The inhibition efficiency of ATA was evaluated by impedance measurements using the following relation:

$$E(\%) = (1 - R_T/R'_T) \times 100 \qquad (2)$$

where R_T and R'_T represent the resistance of charge transfer in 1 M HCl and 1 M HCl + 10^{-2} M ATA, respectively. The value of $E(\%)$ obtained is around 91%. This is close to the values estimated by other methods.

4. Discussion

The comparative study of corrosion inhibition of 10^{-2} M triazole-type compounds indicates that ATA has a much more significant effect. This implies that the corrosion inhibition is due to the presence of amino groups in the molecular structure. However, Sathianandhan *et al.* [33] have reported that, at similar concentrations, the inhibition efficiency obtained with benzotriazole is much greater than that obtained with 1,2,4-triazole or ATA at mild steel in different acidic media.

In the presence of ATA, the cathodic Tafel slope is the same for the amorphous electrode in the absence and presence of the organic inhibitor. This indicates that the inhibition of the hydrogen evolution reaction by ATA takes place by a simple adsorption mode and the mechanism of this reaction is the same for the uninhibited and inhibited condition. If the above statement is valid, the inhibited apparent corrosion rate is proportional to the surface area not covered by ATA and the fraction of surface covered by adsorbed molecules of ATA, Θ, was expressed by the ratio $E(\%)/100$. The relation $\log(\Theta/1-\Theta)$ and $\log C$ where C is the inhibitor concentration, is linear as shown in Fig. 7. Thus the adsorption of ATA obeys

Table 3. Electrochemical galvanostatic impedance parameters of the amorphous FeBSiC alloy in 1 M HCl and in 1 M HCl + 10^{-2} M ATA

Electrolyte	*'HF' loop*			*'LF' loop*		
	f_{HF} /Hz	R_{HF} /Ω cm^2	C_{HF} /μF cm^{-2}	f_{LF} /Hz	R_{LF} /Ω cm^2	C_{LF} /μF cm^{-2}
1 M HCl	–	–	–	0.8	300	70
1 M HCl + 10^{-2} M ATA	10^4	20	0.8	1.0	3000	50

a Langmuir isotherm model

$$\frac{\Theta}{1-\Theta} = kC\exp\left(\frac{-\Delta G}{RT}\right) \qquad (3)$$

where ΔG is the heat of adsorption, k = Constant and C the inhibitor concentration. This isotherm can be used because of the surface homogeneity of the amorphous alloy. For crystalline copper–nickel alloy, which displays surface heterogeneities, the adsorption of ATA has been shown to correspond to the Temkin isotherm model [42]. The value of the free energy of adsorption as calculated from the Langmuir type adsorption isotherm is -40.1 kJ mol^{-1}. The large negative value of ΔG indicates that ATA is strongly adsorbed on the metal surface.

Electrochemical impedance measurements showed two distinct capacitive loops in the presence of ATA. Analysis of the parameters associated with the high frequency loop led us to attribute this loop to the formation of a relatively thick and compact 3D inhibitor film at the surface of the electrode, similar to a paint or polymer film. Similar behaviour was reported by Taib Heakl and Haruyama [43] on copper in 3% NaCl containing benzotriazole and by Srhiri *et al.* [44] on carbon steel XC38 in 3% NaCl with orthoaminothiophenol. Using this hypothesis in the ATA case, the 'LF' loop may be attributed to faradic processes occurring on sites where the ATA film is defective. The ATA inhibitory action may then be attributed to the formation of a thick and relatively compact film at the alloy surface.

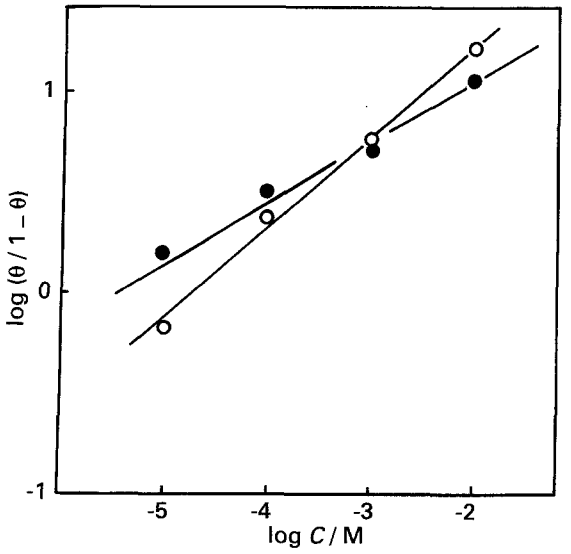

Fig. 7. Langmuir isotherm adsorption model of ATA on the surface of amorphous FeBSiC alloy in 1 M HCl: (○) electrochemical results; (●) gravimetric results.

An attempt was made to correlate ATA electrochemical behaviour and its molecular structure. Nevertheless, no *N*-substituted 1,2,4-triazole type-organic compounds present a planar structure and tend to exist in different tautomeric forms resulting from the non-localized hydrogen of the triazole cycle [45, 46]. ATA is a weak base and its pK_b is 10.8. The pK_b value was determined by titration of a 10^{-2} M ATA solution by 10^{-2} M HCl. Hence, ATA product exist in 1 M HCl (pH 0) in its protonated form. In this case the four tautomeric forms are:

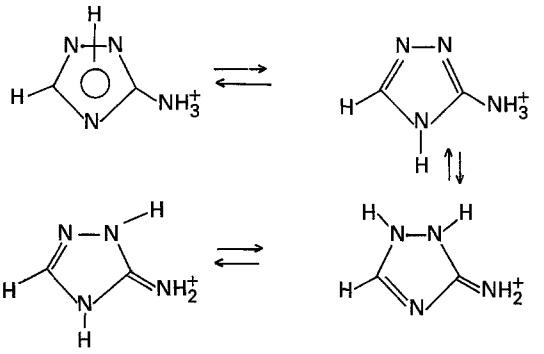

The adsorption of the protonated form of ATA is favoured by the attractive interaction between the Cl^- anions adsorbed and the cations of the inhibitor. This synergic effect was already observed in acid solutions containing Cl^-, I^-, Br^- and inhibitor cations as quaternary ammonium [47], pyridimium ions [48] and amines [49].

When the different models of ATA adsorption are considered, the following models are possible:

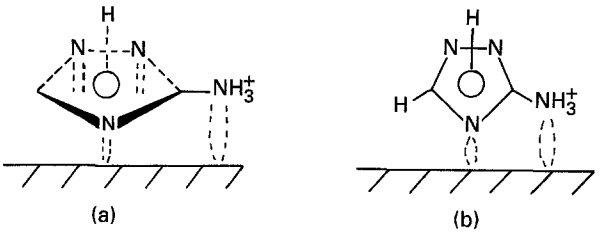

The flat model (a) is stable and preferred since the covered fraction of surface is high, even at low concentrations, and thus explains the cathodic effect of the ATA. This adsorption model is favoured by establishing 'donor–acceptor' links between the empty d orbitals of iron and the pairs of free electrons on the nitrogen atoms and by the electrostatic interactions between NH_3^+ and the adsorbed Cl^- anions on the surface.

The increase in surface coverage with increase in concentration may be illustrated by the following representation:

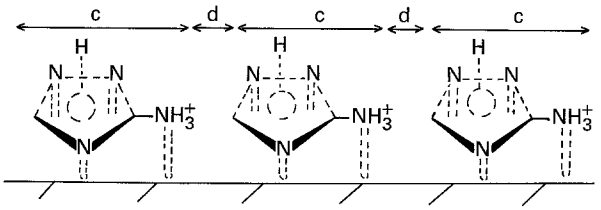

In this case two pictures of the surface may be envisaged:

(i) A fraction of the surface is covered by adsorbed ATA molecules with cathodic and anodic sites.

(ii) The non-covered surface is in direct contact with the electrolyte. On this fraction of electrode surface the hydrogen reduction reaction occurs, confirming the non-modification of their mechanism upon addition of ATA.

The adsorption of ATA, which gives rise to excellent corrosion inhibition must necessarily be followed by molecular stacking on the surface. This leads to the establishment of a stable and relatively thick 3D inhibition layer as follows:

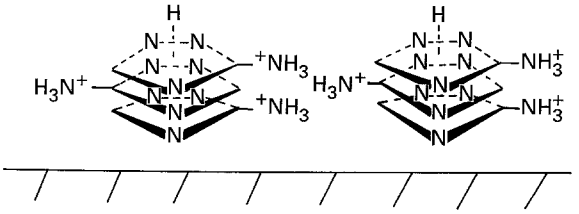

Attempts at preparing a polymer film by electropolymerization of ATA at the surface of amorphous FeBSiC alloy, iron, carbon steel, nickel and copper have led to satisfactory results. The polymer coating obtained exhibits an insulating behaviour. The effect of the polymer coating on corrosion of these metals has been patented [50] and described in the literature [51, 52].

5. Conclusions

The following conclusions can be drawn:

(i) Steady-state measurements have shown that added triazole-type organic compounds do not change the proton reduction mechanism and the corrosion inhibition efficiency of these products can be classified in the following order: ATA > BZT > TR.

(ii) The ATA acts as cathodic inhibitor without modifying the mechanism of the hydrogen evolution reaction.

(iii) The corrosion inhibition efficiency of ATA increases with the inhibitor concentration and reaches a maximum value at 10^{-2} M.

(iv) The cathodic corrosion inhibition of ATA is interpreted by partial blocking of the electrode surface due to adsorption of protonated species according to the Langmuir isotherm on the surface. Hydrogen reduction occurs on the electrode surface which is not covered by the film of ATA.

(v) Electrochemical impedance measurements show that ATA acts through the formation of a 3D film, similar to a paint film at the electrode surface.

(vi) A model for surface coverage of the alloy by ATA is proposed. This model demonstrates the effect of ATA as corrosion inhibitor.

References

[1] P. Duwez and S. C. H. Lin, *J. Appl. Phys.* **38** (1967) 4096.
[2] H. Jouve and G. Nicolas, 21ème colloque de métallurgie. INSTN–CEN Saclay, France (1978) p. 437.
[3] G. J. Sellers, 'Metglass alloys: an answer to low frequency magnetic shielding' European EMC, Symposium, Montreux, Switzerland (1977).
[4] N. Tsura, K. I. Arai and M. Yamada, 'Physica 86–88B' (1977) p. 775.
[5] T. Matsumoto and H. Kimura, *J. Jpn Inst. Metals* **39** (1975) 133.
[6] C. A. Pampillo, *J. Mater. Sci.* **10** (1975) 1194.
[7] T. Masumoto and R. Maddin, *Acta Metall.* **19** (1971) 725.
[8] M. Naka, K. Hashimoto and T. Masumoto, *J. Jpn. Inst. Metals* **38** (1974) 835.
[9] *Idem, J. Cryst. Solids* **28** (1978) 403.
[10] T. P. Moffat, W. F. Flangan and B. D. Lichter, *Corrosion* **43** (1978) 590.
[11] K. Hashimoto, in Amorphous Metallic Alloys, Ed by T. E. Luborsky, Butterworth, London (1983) p. 471.
[12] S. Virtanen and H. Bohni, *Corros. Sci.* **31** (1990) 333.
[13] J. Crousier, J. P. Crousier, Y. Massiani and C. Antonione, *Gazzetta Chimica Italiana* **113** (1983) 329.
[14] M. Da Cunha Belo B. Rondot, E. Navarro, *Métaux Corrosion Industrie* **658** (1980) 02.
[15] M. M. Elsabah, A. A. Baghat and E. E. Saisha, *Corros. Sci.* **25** (1985) 1069.
[16] M. Janik-Czachor, *J. Electrochem. Soc.* **132** (1985) 306.
[17] M. Naka, K. Hashimoto and T. Masumoto, *Corrosion* **36** (1980) 679.
[18] R. B. Diegle, *ibid.* **35** (1979) 250.
[19] K. Asami, M. Naka, K. Hashimoto and T. Masumoto, *J. Electrochem. Soc.* **127** (1980) 2130.
[20] M. D. Archer, C. C. Corke and B. H. Harji, *Electrochim. Acta* **32** (1987) 13.
[21] S. Virtanen, B. Elsener and H. Boehni, *J. Less-Common Metals* **145** (1988) 581.
[22] Y. Waseda and K. Aust, *J. Mat. Sci.* **15** (1981) 2337.
[23] K. Hashimoto, M. Naka and T. Masumoto, *Corrosion* **32** (1976) 146.
[24] T. M. Devine, *J. Electrochem. Soc.* **124** (1977) 38.
[25] R. Wang and M. O. Mrez, *Corrosion* **40** (1984) 272.
[26] K. Asami, K. Hashimoto, T. Masumoto and S. Shimodaria, *Corros. Sci.* **16** (1976) 909.
[27] K. Hashimoto, K. Osada, T. Masumoto and S. Shimodaria, *ibid.* **16** (1976) 71.
[28] S. Kertit, J. Aride, A. Ben Bachir, A. Srhiri, A. Elkholy and M. Etman, *J. Appl. Electrochem.* **19** (1989) 83.
[29] A. Elkholy, M. Etman, S. Kertit, J. Aride, A. Ben Bachir and A. Srhiri, *ibid.* **19** (1989) 512.
[30] M. Etman, A. Elkholy, J. Aride, T. Biaz and S. Kertit, *J. Chim. Phys.* **86** (1989) 347.
[31] J. Aride, A. Ben Bachir, K. El-Kacemi, M. Etman, S. Kertit and A. Srhiri, *ibid.* **88** (1991) 631.
[32] S. Kertit, A. Srhiri and M. Etman, *J. Appl. Electrochem.* **23** (1993) 1132.
[33] B. Sathianandhan, K. Balkrishnan and N. Subramanyan, *Br. Corr. J.* **5** (1970) 270.
[34] N. Eldakar and K. Nobe, *Corrosion* **32** (1976) 238.
[35] *Idem, ibid.* **36** (1981) 271.
[36] P. G. Fox and P. A. Bradley, *Corros. Sci.* **20** (1980) 43.
[37] J. W. Schultze and K. Wipperman, *Electrochim. Acta* **32** (1987) 823.
[38] J. B. Cotton and I. R. Scholes, *Br. Corros. J.* **2** (1967) 1.

[39] G. Lewis, *Corros. Sci.* **22** (1982) 579.
[40] A. Caprani, I. Epelboin, Ph. Morel and H. Takenouti, 4th European Symposium on Corrosion Inhibitors, Ferrara, Italy (1975) p. 571.
[41] I. Epelboin, M. Keddam and H. Takenouti, *J. App. Electrochem.* **2** (1972) 71.
[42] A. Laachach, Thèse 3è Cycle, Rabat, Morocco, (1991).
[43] F. El Taib Heakl and S. Haruyama, *Corros. Sci.* **20** (1980) 887.
[44] A. Srhiri, M. Etman and F. Dabosi, *Werkst. Korros.* **43** (1992) 406.
[45] M. Saidi Idrissi, P. Lannane and C. Garrigou-Lagrange, *J. Chim. Phys.* **78** (1981) 510.
[46] S. Zaydoun, M. Saidi Idrissi and C. Garrigou-Lagrange, *Spectrochim. Acta* **44** (1988) 1421.
[47] R. Driver and R. J. Meakins, *Br. Corros. J.* **9** (1974) 233.
[48] L. I. Antropov, I. S. Pogrebova and G. I. Dremova, *Soviet Electrochem.* **8** (1972) 105.
[49] N. Hackerman, E. S. Snavely and J. S. Payne, *J. Electrochem. Soc.* **113** (1966) 677.
[50] S. Kertit, A. Srhiri, A. Ben Bachir, J. Aride and M. Etman, *Morrocan Patent* 22 994 (1992).
[51] S. Kertit, J. Aride, A. Srhiri, A. Ben Bachir, K. Elkacemi and M. Etman, *J. App. Electrochem.* **23** (1993) 835.
[52] S. Kertit, J. Aride, A. Srhiri, A. Ben Bachir and M. Etman, *C.R. Acad. Sci. Paris*, Série II, **317** (1993) 1399.